SMOOTHED PARTICLE HYDRODYNAMICS SIMULATION OF FUEL TANK SLOSHING

Robert Banim*, Rob Lamb** & Melissa Bergeon**
*BAE SYSTEMS, ATC, Filton, Bristol, UK. **Airbus, Filton, Bristol, UK.

Abstract

The Smoothed Particle Hydrodynamics (SPH) meshless technique has been used to compute the transient flow field and wall pressures resulting from fuel slosh in a 2-dimensional model of a partially full wing tank.

The simulations show the movement of the fuel and location and magnitude of peak wall pressures. Compared to mesh-based CFD methods the solution time is reduced and break up of the free surface is naturally handled.

1 Introduction

1.1 Problem description

The purpose of this work was to investigate the application of the Smoothed Particle Hydrodynamics (SPH) method to simulate the effect of fuel sloshing in the span wise and vertical directions in a typical outer wing tank.

In the work described here, a 2-dimensional model was created from a cross section in a vertical plane through a fuel tank along the span wise direction. Airbus provided accelerations based on a generic interpretation of the accelerations encountered in a limit gust. The SPH code has been used to compute the transient movement of the fuel and forces on the tank walls for a 30% full tank and a 80% full tank.

In Section 2 the tank geometry, accelerations and SPH model set up are described. Section 3 presents the results for the two fill levels. Sections 4 and 5 discuss the results and present the conclusions.

1.2 SPH solution method

Most computational techniques for modelling fluids and solids in finite element (FE) and Computational Fluid Dynamics (CFD) codes require the volume or body to be divided into a grid, or mesh of elements. The governing equations are then approximately solved, by replacing infinitesimal steps in space with these finite-sized elements.

Although such methods are widespread and extensively developed, they have some drawbacks:

- Creating meshes requires human intervention, and ties up substantial effort, particularly with complex CAD.
- In Lagrangian meshes, warping of the elements' shapes can greatly reduce accuracy. Since elements are connected to their immediate neighbours, excessive deformation can tangle the mesh.
- In Eulerian and Lagrangian methods, material breakage and free surfaces are difficult to simulate.

These problems can be circumvented by re-meshing every so often during the simulation. This requires algorithms that automatically adjust or replace the mesh. Re-meshing adds to the computational expense and often introduces numerical errors. Alternatively, a free surface can be tracked using a tracking algorithm such as volume of fluid (VOF) or level set techniques. These techniques are also costly, incur numerical dissipation and tend to smear out the free surface. Further, the break up of the

free surface into many fragments or coalescence cannot be easily modelled.

So called meshless methods do not suffer these drawbacks – there is no mesh to generate or move and free surfaces and material break up are naturally handled. The SPH meshless method was first proposed in 1977 simultaneously by Lucy [1] and Gingold and Monaghan [2]. Recent reviews of the SPH method are given in Li and Liu [3] and Monaghan [4]. The application of SPH to incompressible, free surface flows was first undertaken by Monaghan [5], with validation against a bore and wave problems. Since, the SPH technique has been used to model free surfaces flows by Cleary *et al* [6] and Roubtsova and Kahawita [7], amongst many others and specifically sloshing by Colagrossi [8] and Colagrossi *et al* [9,10].

The BAE SYSTEMS Advanced Technology Centre has an in-house SPH code that has been developed to solve industrial flow problems. The underlying SPH method used is taken from Monaghan [5], details are given by Cleary *et al*, [11]. In summary, the strong form of the governing equations (1,2) is discretised by a collocation technique using an interpolant or smoothing kernel $W(\mathbf{r}, h)$, where $\mathbf{r}$ is position and h the smoothing length.

$$\frac{D\rho}{Dt} = -\rho(\nabla . \mathbf{v}) \qquad (1)$$

$$\rho \frac{D\mathbf{v}}{Dt} = -\nabla P + \frac{1}{3}\nabla(\mu\nabla . \mathbf{v}) + \nabla . (\mu\nabla \mathbf{v}) + \rho\mathbf{g} \qquad (2)$$

The continuous and discrete definitions of the SPH averaging operator on some function *A*, are given in (3) and (4).

$$A_I(\mathbf{r}) = \int A(\mathbf{r}')W(\mathbf{r} - \mathbf{r}', h)d\mathbf{r}' \qquad (3)$$

$$\approx \nabla A(\mathbf{r}) = \sum_b m_b \frac{A_b}{\rho_b}\nabla W(\mathbf{r} - \mathbf{r_b}, h) \qquad (4)$$

The interpolating points may be thought of as particles each carrying a mass *m*, and a velocity **v**. The SPH kernel used here is spline

based and vanishes for separations $> 2h$. This means that summations involve only near neighbours. By implementing an efficient grid based search algorithm that scales linearly with the number of particles, fast solutions are obtained, vindicating the approach under the criteria put forward by Idelsohn and Oñate, [12].

The SPH discrete equations of motion are given by (5-6), where the notation $W(\mathbf{r}_a - \mathbf{r}_b, h) = W_{ab}$ has been used.

$$\frac{d\rho_a}{dt} = \sum_b m_b(\mathbf{v}_a - \mathbf{v}_b)\cdot\nabla_a W_{ab} \qquad (5)$$

$$\frac{d\mathbf{v}_a}{dt} = -\sum_b m_b\left(\frac{P_a}{\rho_a^2} + \frac{P_b}{\rho_b^2} + \Pi_{ab}\right)\nabla_a W_{ab} + \mathbf{F}_a \qquad (6)$$

$\prod_{ab}$ is the viscous term given by Cleary, [13]. The form of the continuity equation used in (5) ensures that there is no smoothing of density at the free surface whilst the momentum equation (6) is written in symmetrized from to conserve linear and angular momentum.

The equation of state used in this simulation is given in (7).

$$P = P_o\left[\left(\frac{\rho}{\rho_o}\right)^\gamma - 1\right] \qquad (7)$$

where $\gamma = 7$ for the fuel. P_o is defined to limit the maximum fluid compression to less than 1% as described by Monaghan, [5].

2 Geometry and Loads

2.1 Model geometry

A 2-dimensional representation of a port wing tank was modelled, as shown in Figure 1. The tank has a length to height ratio of 18 and is split into 10 compartments by vertical wing ribs.

z-direction
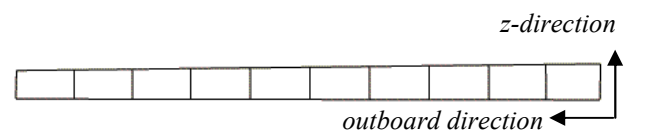

outboard direction

Fig. 1   2-d tank geometry

Flow paths between the compartments at the upper and lower stringer castellations are modelled by introducing gaps of representative size where the ribs meet the upper and lower tank surfaces. These gaps are between 4% and 8% of the rib height. Additionally, there are gaps of similar size representing lightening holes in the four outboard ribs.

2.2 Applied Loads and Boundary Conditions

To represent fuel, the SPH particles were given a density of 817 kg/m^3 and viscosity of 2.2×10^{-3} Pa.s. Particles were created to generate two test cases of 30% and 80% fill levels which required 49333 and 141306 particles respectively.

The two cases were run for 10 seconds to allow the fluid to settle under the applied gravity vector. The gravity vector acts at an angle to the horizontal datum in Figure 1 to account for the dihedral and zero alpha displacement of the wing tank. Figures 2 and 3 show the settled fluid distribution for the two test cases. The particles are coloured by the original compartment they were in before the settling run.

Time varying accelerations due to a limit gust load were then applied to the tank. The accelerations contain a z-direction component perpendicular to the tank major axis and a component along the tank major axis due to the centripetal acceleration. Both components sinusoidally decay, the z-direction component is an order of magnitude greater than the centripetal acceleration.
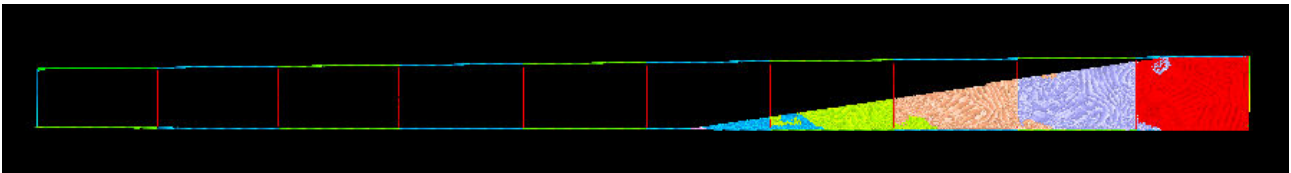

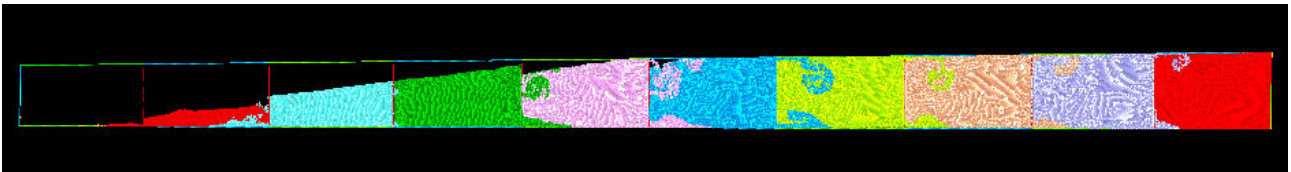Fig. 2   Settled fluid distribution, 30% full level.

Fig. 3   Settled fluid distribtution, 80% fill level.

3 Results

3.1 Sloshing results for 30% full tank

Figures 4 - 6 show the evolution of the fuel location at time intervals; $t = 0.6$ s, 0.9913 s and 1.41 s. The centre of gravity of the fuel at each instant is represented with a red dot. Only the 6 inboard compartments are shown as the fuel does not reach any further outboard.

The pressure on the upper and lower tank walls was also computed by spatially averaging over the segments making up each compartment with a sampling period of 25 ms.

In Figure 7 the pressures on the upper (U) and lower (L) walls are shown for each compartment. The compartments are numbered from C01 at the inboard end to C10 at the outboard end. Note that the pressure values have intentionally been removed although all pressure plots have the same pressure scale increments.

Figure 7 shows that the maximum pressure occurs in compartment C03 at $t = 575$ ms as the downward moving fluid is impacted by the upward accelerating tank. The peak pressure is approximately 50% greater than the pressure in the full compartment C01 where sloshing forces are negligible.
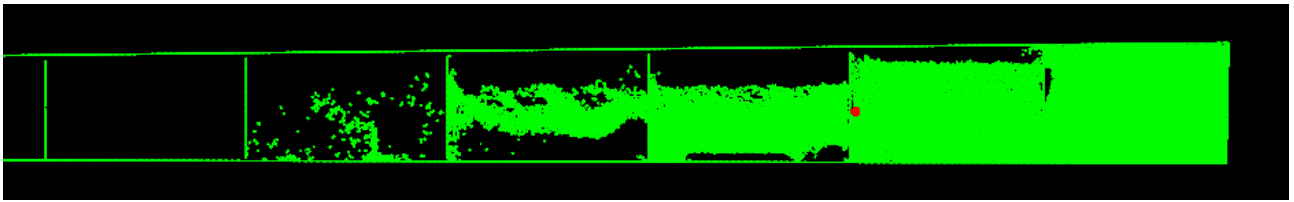
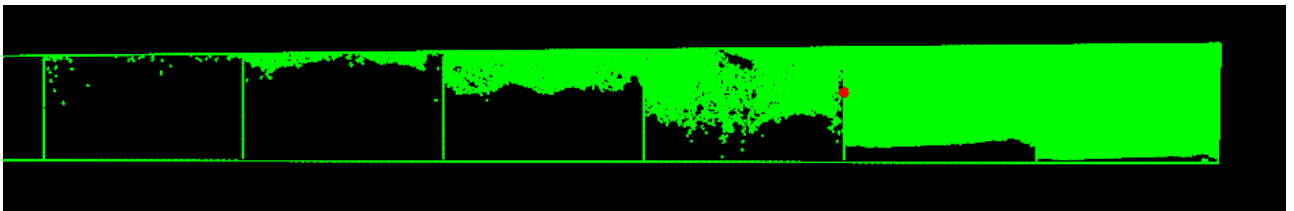Fig 4   30% full tank. Flow solution at *t* = 600ms. Centre of gravity shown as red dot.

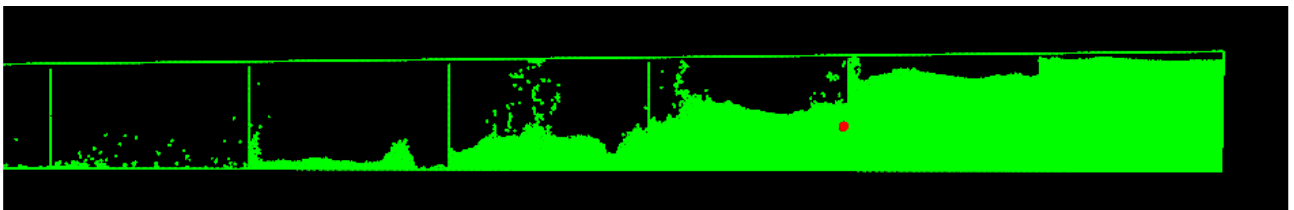Fig 5   30% full tank. Flow solution at *t* = 1000ms. Centre of gravity shown as red dot

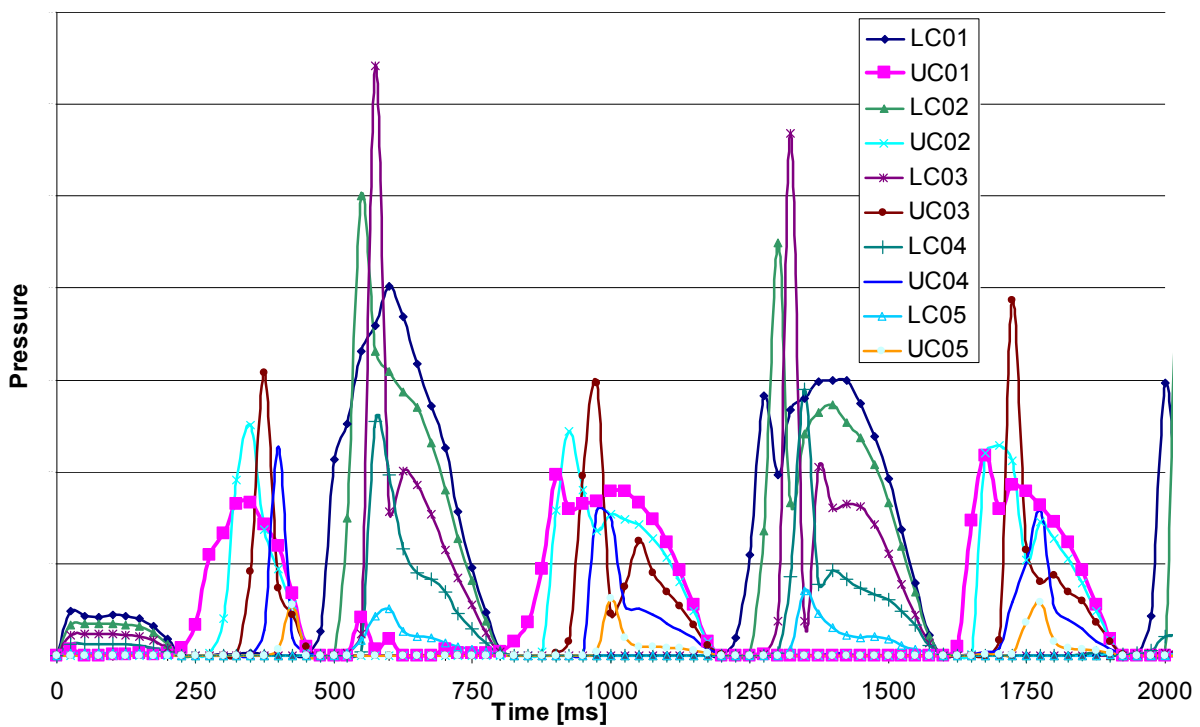Fig 6   30% full tank. Flow solution at *t* = 1000ms. Centre of gravity shown as red

Fig. 7   30% full tank. Pressures on the upper and lower walls for filled compartments.

3.2 Sloshing results for 80% full tank.

Figures 8-10 show the fuel movement for the 80% full tank at the time intervals given in Section 3.1. For this case, all 10 compartments are shown as the fuel reaches the outboard end of the tank.

The average pressure on the upper and lower tank walls for the five inboard compartments (C01 – C05) are shown in Figure 11, Figure 12 shows the pressures on the outboard compartments (C06 – C10).

The wall pressures in the five inboard compartments are similar since these compartments are full of fuel so sloshing forces are small. They agree with the analytic solution for the case of a full tank of incompressible fluid as shown in Section 4.

For the partially full outboard compartments, Figure 12 shows that the highest peak pressure is in compartment C07 at $t = 575$ ms. The peak pressure is approximately 35% greater than the pressure for the full compartments.
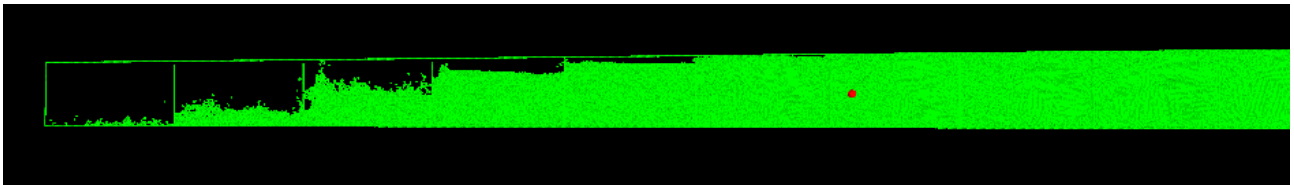

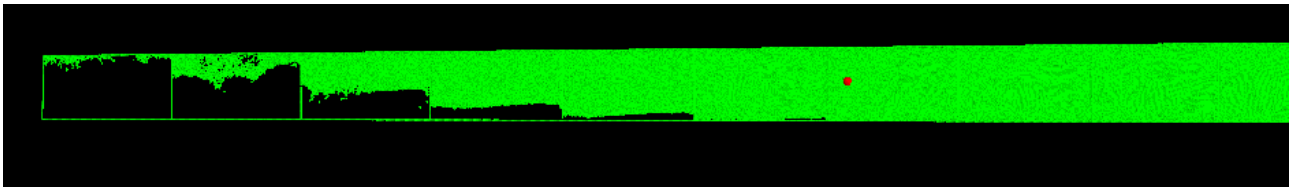Fig 8   80% full tank. Flow solution at $t = 600$ms. Centre of gravity shown as red dot.

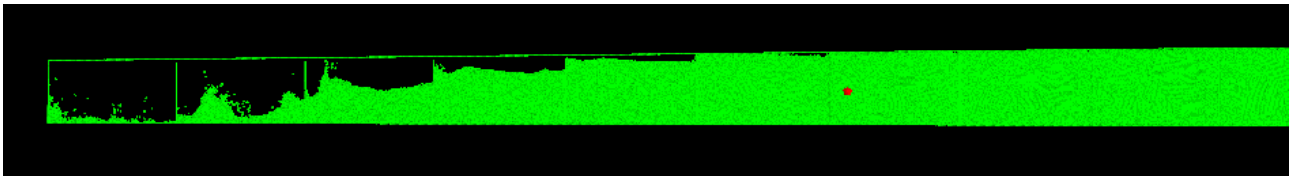Fig 9   80% full tank. Flow solution at $t = 1000$ms. Centre of gravity shown as red dot

Fig 10   80% full tank. Flow solution at $t = 1000$ms. Centre of gravity shown as red
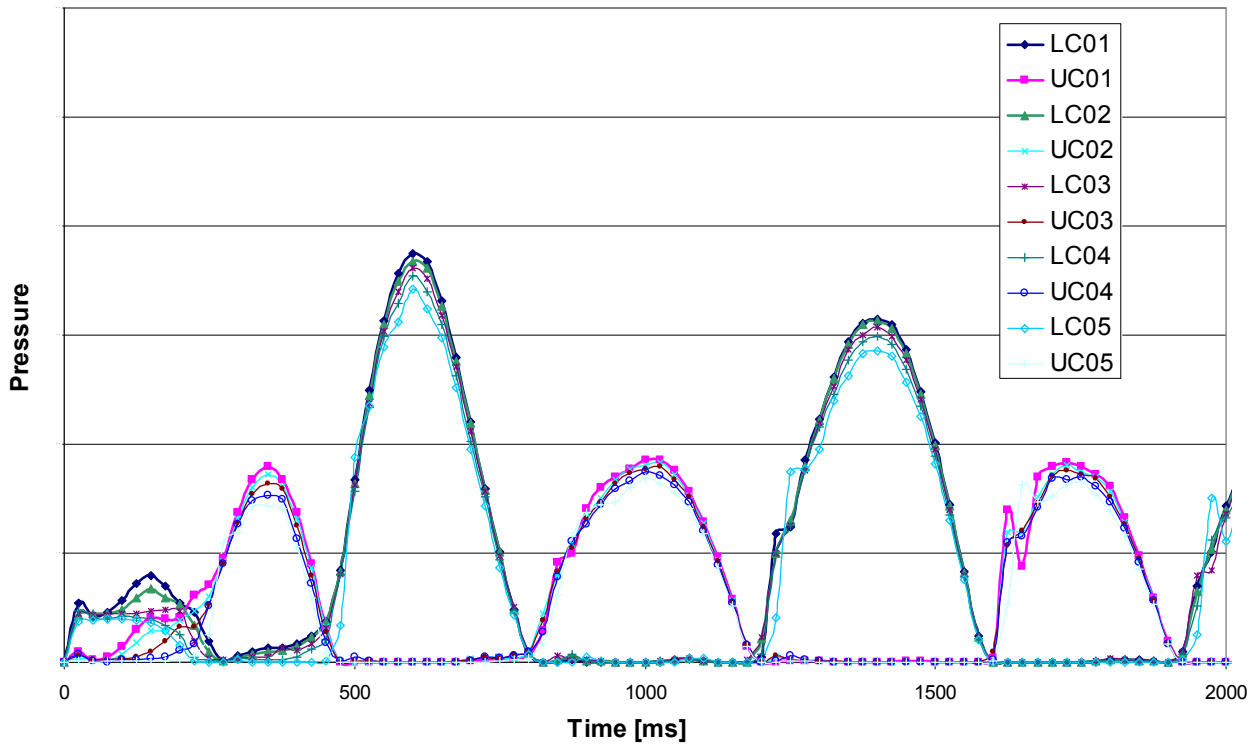
Fig. 11   80% full tank. Pressures on upper and lower surfaces of compartments C01 – C05.
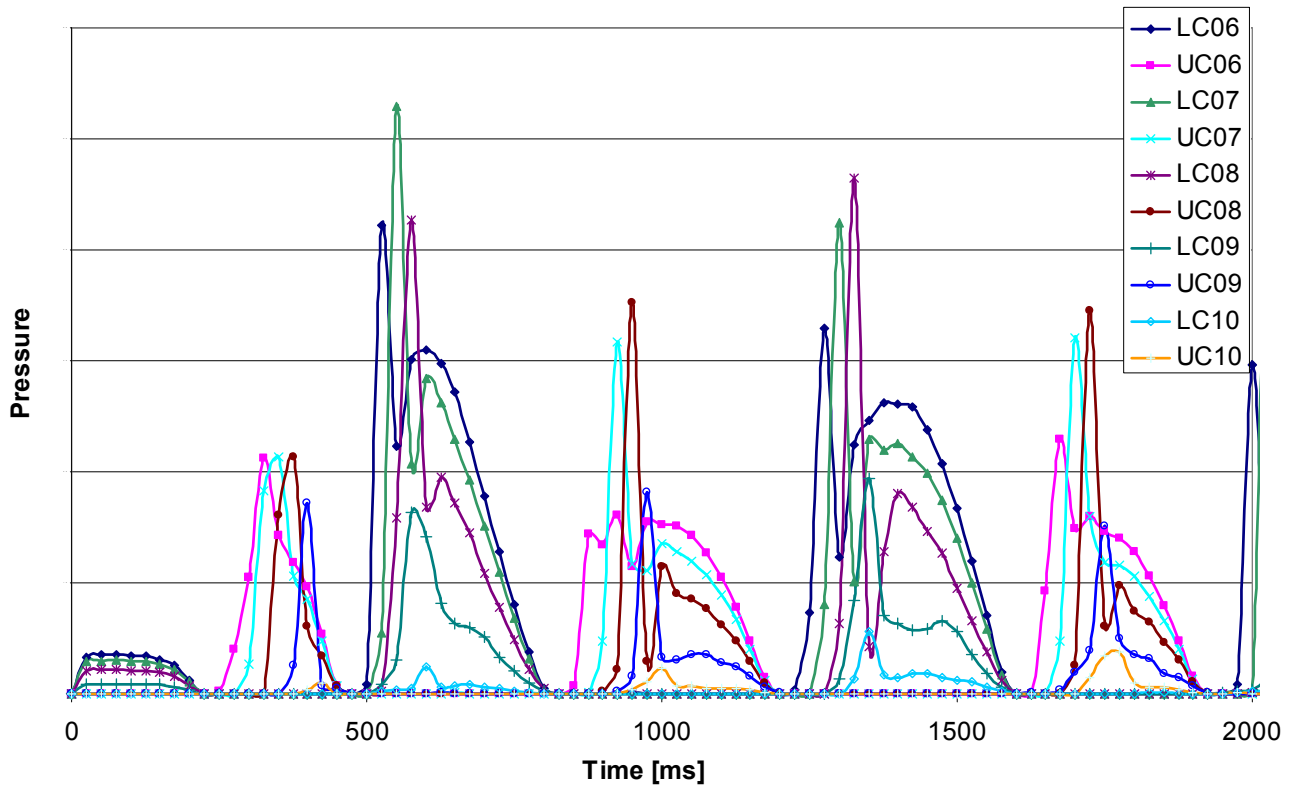

Fig. 12   80% full tank. Pressures on upper and lower surfaces of compartments C06 – C10.
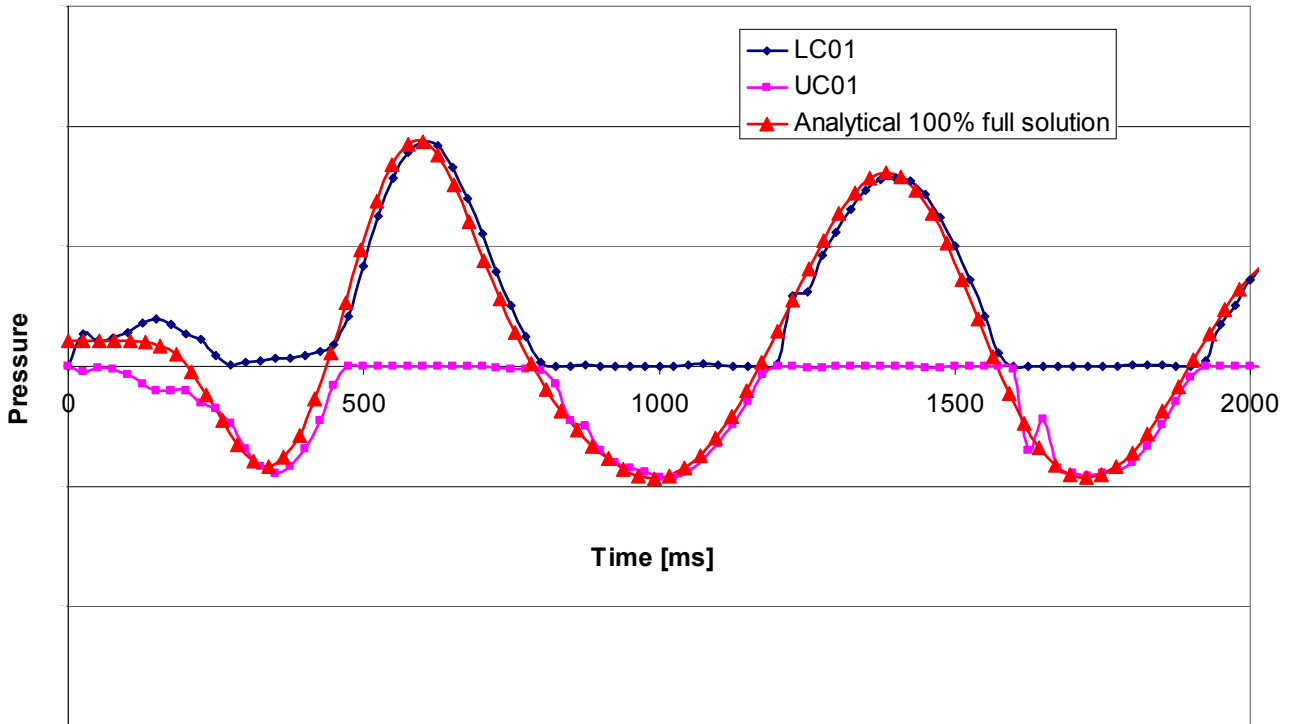
Fig. 13   Comparison of SPH pressures and analytical solution in C01 for 100% full compartment.

4 Discussion

To give some confidence in the accuracy of the SPH generated sloshing forces it is useful to compare the SPH solution with a simple analytical solution for any of the 100% full compartments.

For this comparison the spanwise acceleration component and spanwise flow have been neglected so that for an incompressible fluid the pressure on the upper or lower wall is simply given by:

$$P = (m_c \times a) / w \qquad (8)$$

where m_c is the mass of fluid, a is its acceleration and w is the compartment width.

Figure 13 shows that excellent agreement is obtained between the analytic solution and the SPH solution for compartment C01. (The pressure on the upper wall, UC01, has been multiplied by -1 to represent a downward force). Similar results can be obtained for the

other full compartments. As well as validating the method of obtaining wall pressure from the Lennard-Jones particle forces, this result also shows that there is no significant error introduced by using a pseudo-incompressible formulation..

For a given exciting acceleration and frequency, there is a certain fuel fill level within a compartment that will give a maximum sloshing force as the inertia of the fuel is reversed by the tank walls. For the 30% full case, the peak pressure occurs in compartment C03 which is 57% full. In the 80% full case compartment C07 is 83% full when the maximum peak pressure occurs. Given relatively short run times (24 hours on a high end PC for 5 seconds of sloshing with the 80% full case) of the SPH technique, it is feasible to iterate with different fill levels and geometry. This allows either design optimisation or worst case scenarios to be investigated.

For the test data used, the effect of the centripetal acceleration is to gradually increase

the mass of fuel in the outboard compartments. Due to the decaying nature of the z-acceleration, the peak pressures on the tank walls are obtained early in the response, before there is significant outboard movement.

Similar peak pressures over the first second would have been obtained if the centripetal acceleration and span wise flow had been neglected. This suggests that the SPH model could be run at a much larger particle spacing as the holes in the ribs would not need to be resolved. This would make it possible to run a full 3-D model without much extra computational cost.

5 Concluding Remarks

The BAE SYSTEMS SPH code has been used to model sloshing in a wing fuel tank. With this technique, problem setup was straight forward with no requirement to generate a volume mesh. Run times were also fast in comparison to Eulerian methods with interface tracking algorithms.

The SPH code generated animations of fuel movement that showed the complex nature of the sloshing behaviour featuring break-up and coalescence of the free surface. The Lennard-Jones wall forces were extracted and used to analyse the peak sloshing pressures exerted by the fuel.

Whilst the work presented here was for a 2-dimensional test case, other 3-dimensional sloshing problems with complex geometry have been analysed using the BAE SYSTEMS SPH code for automotive and aerospace applications. In these problems tank geometry and fuel pick-up positions have been optimised.

Further improvements in code run time could be made by using new hardware accelerator technology or an efficient distributed memory parallel version of the code. A variable resolution scheme that could reduce the number of particles whilst maintaining the speed of the current near neighbour search algorithm would also be a desirable development.

6 References

[1] Lucy L.B. A Numerical Approach to the Testing of the Fission Hypothesis. *Aston. Jn. No.* 82, pp 1013-1024, 1977.

[2] Gingold R.A. & Monaghan J.J. Smoothed Particle Hydrodynamics: theory and application to non-spherical stars. *Mon. Not. R. Astron. Soc.,* No. 181, pp 375-389, 1977.

[3] Li S. & Liu W.K. Meshfree and particle methods and their applications. *Appl. Mech. Rev.,* Vol. 55, No. 1, pp 1 – 34, 2002.

[4] Monaghan J.J. Smoothed Particle Hydrodynamics. *Rep. Prog. Phys.* No. 68, pp 1703 – 1759, 2005.

[5] Monaghan J.J. Simulating Free Surface Flows with SPH. *Journal of Computational Physics* No. 110, pp 399-406, 1994.

[6] Cleary P., Prakash M., Ha J., Stokes N. & Scott C. Smooth Particle Hydrodynamics: Status and future Potential. *Proc. 4th Int. Conf. on CFD in the Oil and Gas, Metallurgical & Process Industries,* SINTEF/NTNU, Trondheim, Norway, pp 1 – 21, 2005.

[7] Roubtsova V. & Kahawita R. The SPH technique applied to free surface flows. *Computers & Fluids,* in press May 2006 (available on-line at www.elsevier.com/locate/compfluid).

[8] Colagrossi A. Dottorato di Ricerca in Meccanica Teorica ed Applicata CICLO. A meshless Lagrangain method for free-surface and interface flows with fragmentation. *PhD Thesis,* Universita di Roma, La Sapienza, 2004.

[9] Colagrossi A. & Landrini M. Numerical Simulation of interfacial flows by SPH. *J. Comp. Phys.* No 191, pp 448-75, 2003.

[10] Colagrossi A., Lugni C., Douset V., Bertram V. & Flatinsen O. Numerical and experimental study of sloshing in partially filled rectangular tanks. *6th Numerical Tank Towing Symp.* Rome, Italy, 2003.

[11] Cleary P., Stokes N., Monaghan J. & Prakash M. Smoothed Particle Hydrodynamics Theory Manual Issue 2. *BAE SYSTEMS Australia SPH Report.* No SPH/1377/010, 2002.

[12] Idelsohn S.R. & Oñate E. To mesh or not to mesh. That is the question…*Comp. Meth. In applied mechanics and engineering.* In Press May 2006. (available on-line at www.elseviercom/locate/cma)

[13] Cleary P., SPH Tech Note #8 New Implementation of viscosity. *CSIRO Division of Mathematics and Statistics Tech Report.* No. DMS – C96/32, 1996.